Dark Matter Phenomenology in Triplet Extensions of the Standard Model

Submitted by: Niharika Shrivastava (21187)

Supervisor: Dr. Rahul Srivastava

Affiliation: Indian Institute of Science Education and Research (IISER) Bhopal

This report will cover study of dark matter phenomenology in Standard Model extensions containing an electroweak triplet field, where the triplet can be either a scalar or a fermion with hypercharge $Y = 2$. These minimal triplet extensions provide well-motivated Dark Matter candidates stabilized by the $\mathbb{Z}_2$ discrete symmetry. We perform a detailed analysis of the parameter space consistent with current cosmological and experimental constraints, including the relic abundance and direct detection limits. For future work, we will analyse the indirect detection and collider phenomenology and compare the models for their hypercharge assignment and present if triplet can be viable candidate or if we can rule out this possibility.

1. INTRODUCTION

One of the landmark accomplishments in twentieth-century physics is the formulation of the Standard Model (SM) of particle physics. This framework provides a unified, self-consistent, and remarkably successful description of the fundamental particles and their interactions.

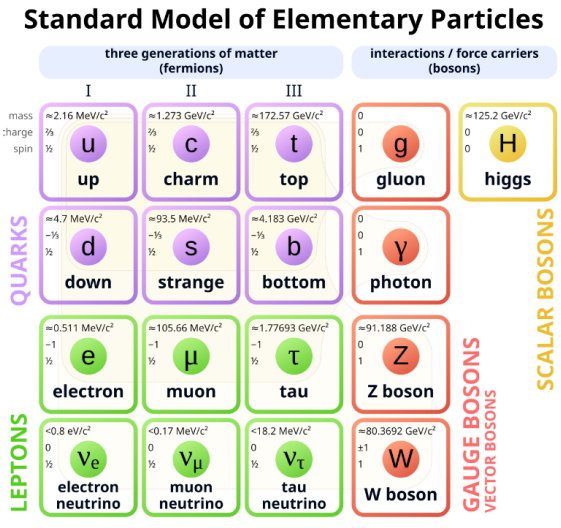

FIG. 1: Particle content of the SM

The particle nature of dark matter has remained one of the central puzzles in modern physics since the first observations of galaxy rotation curves. Current cosmological observations (Planck) indicate that the energy budget of the Universe is dominated by dark energy and dark matter, with approximate fractions of 69% dark energy, 26% dark matter and 5% baryonic matter [1]. This makes it evident that we need to extend the SM in order to incorporate DM and its interactions with visible matter.

To extend SM, we will add new particles and impose an extra symmetry for the stability of the DM candidate. Here, we have considered two cases, one in which we have added a scalar triplet and another in which we have added fermionic triplet. We will perform the relic density calculation and direct detection searches in order to find out how these models will perform to current experimental data. Firstly, we will begin with a brief introduction of DM and its candidates.

2. DARK MATTER

Dark Matter differs fundamentally from ordinary matter in that it does not couple to electromagnetic interactions. Consequently, it neither absorbs nor emits electromagnetic radiation, rendering it invisible to conventional detection methods. Our knowledge of DM's existence derives solely from its gravitational influence on observable matter. Primary evidence for DM arises from its gravitational effects on the dynamics of galaxies and galaxy clusters. Additional indirect probes include observations of the Cosmic Microwave Background radiation and weak gravitational lensing phenomena. The current scientific focus has shifted from establishing DM's existence to determining its fundamental nature—investigating whether it manifests as a particle species, a fluid-like medium, or an entirely novel physical entity.

2.1. Dark Matter Candidates

DM candidates span an enormous parameter space, with proposed masses varying across multiple orders of magnitude and interaction strengths with baryonic matter ranging from extremely weak to vanishingly small. Below are some of the leading theoretical candidates:

a. ***Weakly Interacting Massive Particles (WIMPs)*** are hypothetical particles with masses typically in the GeV–TeV range that interact via the weak nuclear force. They naturally achieve the observed relic abundance through the thermal "freeze-out" mechanism, making them one of the most studied DM candidates.

b. ***Feebly Interacting Massive Particles (FIMPs)*** are very weakly coupled to the SM. Unlike WIMPs, they never reach thermal equilibrium in the early universe. Their relic density is produced via the "freeze-in" mechanism through the slow decay or annihilation of heavier particles.

c. ***Axions*** are very light pseudo-scalar particles originally proposed to solve the strong CP problem in QCD. They can be produced non-thermally in the early universe via the misalignment mechanism and can behave as cold DM due to their extremely low mass and weak coupling to photons.

d. ***Ultra-light DM*** refers to bosonic particles with masses around 10^{-22}–10^{-18} eV. Such particles have macroscopic de Broglie wavelengths, leading to wave-like effects on galactic scales and potentially resolving small-scale structure problems of cold DM.

e. ***Sterile Neutrinos*** are right-handed neutrinos that interact only via mixing with active neutrinos. keV-scale sterile neutrinos can be produced through oscillations in the early universe and constitute warm DM, influencing structure formation and potentially giving rise to observable X-ray lines.

1. ***WIMPS***

Weakly Interacting Massive Particles (WIMPs) represent the most thoroughly investigated and experimentally pursued class of DM candidates. The motivation behind the WIMP framework lies in the fact that WIMPs can naturally reproduce the observed DM relic abundance through the well-established mechanism of *thermal freeze-out* in the early Universe[2, 3]. This process typically occurs for particles with masses around the electroweak scale, comparable to those of the W and Z bosons. The simplicity of WIMP models, together with their experimentally testable freeze-out signatures and active searches over a broad mass range, has driven a significant amount of theoretical effort toward constructing WIMP-like DM scenarios.

The thermal freeze-out mechanism offers a simple and generic framework for explaining the observed relic DM abundance [4]. If the early Universe reached temperatures near the weak scale, WIMPs would have been efficiently produced, annihilated, and scattered through interactions with SM particles, thereby maintaining *thermal equilibrium*. As the Universe expanded and cooled, these interaction rates eventually dropped below the Hubble expansion rate, causing WIMPs to decouple from the thermal bath. Once the annihilation rate became slower than the expansion rate, the comoving number density of WIMPs effectively froze, marking the *freeze-out epoch*. Subsequent cosmic expansion further diluted their abundance, ultimately leading to the relic DM density observed today.

For a typical WIMP candidate, denoted by χ, freeze-out occurs when the plasma temperature falls to approximately $T \sim m_\chi/25$, where m_χ is the WIMP mass [4]. After accounting for cosmological dilution, the present-day WIMP relic density from thermal freeze-out can be approximated as[5]:

$$\Omega_\chi h^2 \equiv \frac{\rho_\chi}{\rho_c/h^2} \simeq 0.119\,\frac{3\times10^{-26}\,\mathrm{cm}^3/\mathrm{s}}{\langle\sigma v\rangle}, \tag{1}$$

where $\langle\sigma v\rangle$ is the thermally averaged annihilation cross section, and $\rho_c = 3H_0^2/8\pi G$ is the critical density of the Universe. The normalized Hubble parameter is $h = H_0/(100\,\mathrm{km\,s^{-1}Mpc^{-1}}) \simeq 0.7$. For comparison, cosmological observations give $\Omega_\chi h^2 = 0.12 \pm 0.001$ [1]

An important implication of Eq. (1) is that the relic density depends primarily on the annihilation cross section $\langle\sigma v\rangle$. [6]

Search for WIMPs is being pursued through three complementary approaches: direct, indirect, and collider-based experiments(**??**). Direct detection aims to observe nuclear

recoils from WIMP–nucleon scattering in underground detectors such as XENONnT, LZ, and PandaX. Indirect searches look for annihilation or decay products—such as gamma rays, positrons, or neutrinos—from regions of high DM density, using observatories like Fermi-LAT, AMS-02, and IceCube. Collider experiments, particularly at the LHC, attempt to produce WIMPs via missing transverse energy signatures in high-energy collisions. Together, these searches probe different regions of the WIMP parameter space, tightly constraining their mass and interaction cross section.

Motivated by this, we take our extended particles to be WIMP DM candidates. Now we will setup our model by adding new kinetic and interaction terms of DM particles to SM Lagrangian.

3. MODEL SETUP

3.1. Scalar triplet

Gauge Group	Baryon Fields			Lepton Fields		Scalar Fields	
	$Q_L^i = (u_L^i, d_L^i)^T$	u_R^i	d_R^i	$L_L^i = (\nu_L^i, e_L^i)^T$	e_R^i	H	Δ_2
$SU(3)_c$	3	3	3	1	1	1	1
$SU(2)_L$	2	1	1	2	1	2	3
$U(1)_Y$	1/6	2/3	−1/3	−1/2	−1	1/2	2
$\mathbb{Z}_2$	+	+	+	+	+	+	−

TABLE I: Particle content and their corresponding charges under various symmetry groups, with the scalar triplet Δ_2.

We extend the SM by adding a complex scalar triplet with U(1) hypercharge $Y = 2$. The triplet is denoted by Δ_2 and transforms as $(\mathbf{1}, \mathbf{3}, 2)$ under $SU(3)_C \otimes SU(2)_L \otimes U(1)_Y$; the subscript indicates the hypercharge. The triplet contains components with electric charges $+2, +1$, and 0. The particle content and details on additional $\mathbb{Z}_2$ symmetry is shown in table I.

The Lagrangian for the scalar sector is given as

$$\mathcal{L}_{\text{scalar}} = (D_\mu H)^\dagger (D^\mu H) + \text{Tr}(D_\mu \Delta_2)^\dagger (D^\mu \Delta_2) - V(H, \Delta_2) \tag{2}$$

$$\begin{aligned}\mathcal{L}_{\text{scalar}} = (D_\mu H)^\dagger (D^\mu H) + \text{Tr}\big[(D_\mu \Delta_2)^\dagger (D^\mu \Delta_2)\big] \\ - \Big(-\mu^2 H^\dagger H + \mu_{\Delta_2}^2 \,\text{Tr}[\Delta_2^\dagger \Delta_2] + \tfrac{1}{2}\lambda_H (H^\dagger H)^2 + \tfrac{1}{2}\lambda_\Delta \,\text{Tr}[\Delta_2^\dagger \Delta_2 \Delta_2^\dagger \Delta_2] \\ + \tfrac{1}{2}\lambda'_\Delta \Big(\text{Tr}[\Delta_2^\dagger \Delta_2]\Big)^2 + \tfrac{1}{2}\lambda_{H\Delta} H^\dagger H \,\text{Tr}[\Delta_2^\dagger \Delta_2] + \tfrac{1}{2}\lambda'_{H\Delta} H^\dagger (\Delta_2 \Delta_2^\dagger) H \Big)\end{aligned} \tag{3}$$

where,

$$H = \begin{pmatrix} G^+ \\ \frac{1}{\sqrt{2}}(v + h + iG^0) \end{pmatrix}, \quad \Delta_2 = \begin{pmatrix} \Delta_2^1 \\ \Delta_2^2 \\ \Delta_2^3 \end{pmatrix} \tag{4}$$

We can write real triplet in bidoublet form that makes gauge-invariant contraction easy. It can be written in 2×2 matrix representation by expanding them in Pauli matrices as $\Delta_2 = \frac{1}{\sqrt{2}}\sigma_i \Delta^i$,

where σ_i are pauli matrices $\sigma_1 = \begin{pmatrix} 0 & 1 \\ 1 & 0 \end{pmatrix}$ $\sigma_2 = \begin{pmatrix} 0 & -i \\ i & 0 \end{pmatrix}$ $\sigma_3 = \begin{pmatrix} 1 & 0 \\ 0 & -1 \end{pmatrix}$,

$$\Delta_2 = \frac{1}{\sqrt{2}} \begin{pmatrix} \Delta_2^3 & \Delta_2^1 - i\Delta_2^2 \\ \Delta_2^1 + i\Delta_2^2 & -\Delta_2^3 \end{pmatrix} \tag{5}$$

where $\Delta_2^+(Q = +1) \equiv \Delta^3$, $\Delta^{++}(Q = +2) = \frac{\Delta_2^1 - i\Delta_2^2}{\sqrt{2}}$ and $\Delta_2^0(Q = 0) = \frac{\Delta_2^1 + i\Delta_2^2}{\sqrt{2}}$.

Hence, in adjoint representation our triplet becomes,

$$\Delta_2 = \begin{pmatrix} \frac{\Delta_2^+}{\sqrt{2}} & \Delta_2^{++} \\ \Delta_2^0 & -\frac{\Delta_2^+}{\sqrt{2}} \end{pmatrix} \tag{6}$$

with $\Delta_2^0 = \Delta_{2R}^0 + i\Delta_{2I}^0$ and $\Delta_2^0, \Delta_2^+$and Δ_2^{++} are independent fields.

The covariant derivative is defined as :

$$D_\mu \Delta_0 = \partial_\mu \Delta_0 + ig[\tilde{A}_\mu, \Delta_0], \qquad \text{where} \quad \tilde{A}_\mu = \sum_{a=1}^{3} A_\mu^a T^a \tag{7}$$

. The general form of a renormalizable potential is given as follows:

$$\begin{aligned} V(H, \Delta_2) = & -\mu^2 H^\dagger H + \mu_{\Delta_2}^2 \,\mathrm{Tr}(\Delta_2^\dagger \Delta_2) + \frac{1}{2}\lambda_H (H^\dagger H)^2 + \frac{1}{2}\lambda_\Delta \,\mathrm{Tr}(\Delta_2^\dagger \Delta_2 \Delta_2^\dagger \Delta_2) + \\ & + \frac{1}{2}\lambda'_\Delta (\mathrm{Tr}[\Delta_2^\dagger \Delta_2])^2 + \frac{1}{2}\lambda_{H\Delta} H^\dagger H \,\mathrm{Tr}[\Delta_2^\dagger \Delta_2] + \frac{1}{2}\lambda'_{H\Delta} H^\dagger \Delta_2 \Delta_2^\dagger H, \end{aligned} \tag{8}$$

Here, we are imposing a $\mathbb{Z}_2$ symmetry under which all (SM) particles are even and scalar triplet is odd, this symmetry makes the neutral component stable. This symmetry ensures DM particles do not annihilate to SM particles. Following conditions ensures the scalar potential remains bounded from below, preventing vacuum instability in the triplet model[7]:

$$\lambda_H > 0, \lambda_\Delta + \lambda'_\Delta > 0, \lambda'_\Delta + \frac{\lambda_\Delta}{2} > 0$$
$$\lambda_{H\Delta} + \sqrt{2\,\lambda_H(\lambda_\Delta + \lambda'_\Delta)} > 0, \lambda_{H\Delta} + \sqrt{2\,\lambda_H\left(\lambda'_\Delta + \frac{\lambda_\Delta}{2}\right)} > 0,$$
$$\lambda_{H\Delta} + \lambda'_{H\Delta} + \sqrt{2\,\lambda_H(\lambda_\Delta + \lambda'_\Delta)} > 0, \lambda_{H\Delta} + \lambda'_{H\Delta} + \sqrt{2\,\lambda_H\left(\lambda'_\Delta + \frac{\lambda_\Delta}{2}\right)} > 0. \tag{9}$$

The mass for triplet scalar is given as follows

$$\begin{aligned} m_h^2 &= \lambda_H v^2, \\ m^2_{\Delta^0_{2R}} = m^2_{\Delta^0_{2I}} &= M^2 + \tfrac{1}{4}(\lambda_{H\Delta} + \lambda'_{H\Delta})v^2, \\ m^2_{\Delta_2^\pm} &= M^2 + \tfrac{1}{4}\left(\lambda_{H\Delta} + \tfrac{\lambda'_{H\Delta}}{2}\right)v^2 = m^2_{\Delta^0_{2R}\,(\Delta^0_{2I})} - \tfrac{\lambda'_{H\Delta}}{8}v^2, \\ m^2_{\Delta_2^{\pm\pm}} &= M^2 + \tfrac{1}{4}\lambda_{H\Delta}v^2 = m^2_{\Delta^0_{2R}\,(\Delta^0_{2I})} - \tfrac{\lambda'_{H\Delta}}{4}v^2\,. \end{aligned} \tag{10}$$

v is the vacuum expectation value of Higgs.

3.2. Fermionic triplet

Gauge Group	Baryon Fields			Lepton Fields			Scalar Fields
	$Q^i_L = (u^i_L, d^i_L)^T$	u^i_R	d^i_R	$L^i_L = (\nu^i_L, e^i_L)^T$	e^i_R	Σ_2	H
$SU(3)_c$	3	3	3	1	1	1	1
$SU(2)_L$	2	1	1	2	1	3	2
$U(1)_Y$	1/6	2/3	−1/3	−1/2	−1	2	1/2
$\mathbb{Z}_2$	+	+	+	+	+	−	+

TABLE II: Particle content and their corresponding charges under various symmetry groups, with the fermion triplet Σ_2.

Similarly to the analysis of triplet scalar DM, here also extend the SM by taking the hypercharge of the fermionic triplet as Y = 2. Hence, the left handed fermion triplet Σ_2 with charge under $SU(3)_C \otimes SU(2)_L \otimes U(1)_Y \sim (1, 3, 2)$. The particle content and details on additional $\mathbb{Z}_2$ symmetry is shown in table II. By charge calculation for this hypercharge combination for fermion we will get three particles with charges 0, +1 and +2 respectively. Thus, Σ_2 will involve Dirac mass term as it is a complex triplet. Keeping this in mind, we

write the complete Lagrangian:

$$\mathcal{L} = \mathcal{L}_{\rm SM} + \mathcal{L}_{\Sigma_2} \tag{11}$$

The $\mathcal{L}_{\Sigma_2}$ with kinetic and mass terms is expressed as:

$$\mathcal{L}_{\Sigma_2} = \mathrm{Tr}\left[\overline{\Sigma_2}\, i\gamma^\mu D_\mu \Sigma_2\right] - [M\ Tr(\overline{\Sigma}_{2L}(\Sigma_{2R})) + h.c.], \tag{12}$$

Σ_{2L} and Σ_{2R} are left and right phase of the fermionic field. The covariant derivative D_μ is defined by

$$D_\mu = \partial_\mu - ig\, T_i^{\rm adj} W_i, \tag{13}$$

with g being the $SU(2)_L$ gauge coupling, W_i the associated gauge fields, and $T_i^{\rm adj}$ representing the triplet adjoint representation generators. M_{ij} is the mass matrix of the fermion.

The triplet Σ_2 can be written in its fundamental representation as:

$$\Sigma_{2L} = \frac{1}{2}\begin{pmatrix} \Sigma^+ & \sqrt{2}\Sigma^{++} \\ \sqrt{2}\Sigma^0 & -\Sigma^+ \end{pmatrix} \quad , \quad \Sigma_{2R} = \frac{1}{2}\begin{pmatrix} \Sigma^+ & \sqrt{2}\Sigma^{++} \\ \sqrt{2}\Sigma^0 & -\Sigma^+ \end{pmatrix} \tag{14}$$

At tree level all three components are degenerate in mass; radiative (one–loop) corrections lift this degeneracy, typically making the neutral component the lightest and also the dark matter candidate.

4. DM PHENOMENOLOGY

Here, we focus on exploring the particle nature, production mechanisms, and observational signatures of DM beyond the SM of particle physics. This analysis aim to connect these theoretical models with experimental observables by examining their implications for cosmology, astrophysical signals, and collider experiments.We investigate the phenomenological viability of the triplet scalar DM model by performing a systematic scan over the relevant parameter space. Our models contains several dimensionless quartic coupling parameters and one mass parameter, which we constrain as follows:

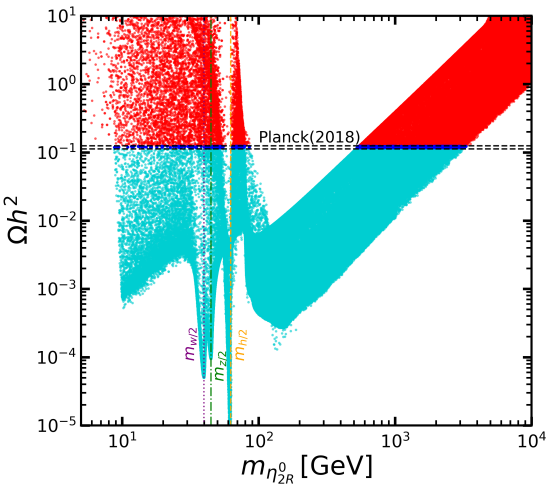

FIG. 2: Relic density for Scotogenic Model

Parameter	Range
λ_H	$[0.2555]$
$\mu^2_{\Sigma_2}$	$[10^2, 10^8]$ GeV^2

(a) Fermion triplet

Parameter	Range
λ_H	$[0.2555]$
λ_Δ	$\pm[10^{-8}, 4\pi]$
λ'_Δ	$\pm[10^{-8}, 4\pi]$
$\lambda_{H\Delta}$	$\pm[10^{-8}, 4\pi]$
$\lambda'_{H\Delta}$	$-[10^{-8}, 4\pi]$
$\mu^2_{\Delta_2}$	$[10^2, 90^8]$ GeV^2

(b) Scalar triplet

TABLE III: Parameter space ranges used in the scan for fermion and scalar triplets.

4.1. Relic Density

Figure 3 illustrates the relic density Ωh^2 of the DM candidate as a function of its mass for the triplet models. The plot reveals three distinct resonance dips at approximately 40 GeV, 45 GeV, and 62.5 GeV, corresponding to DM masses near half the masses of the W boson, Z boson, and Higgs boson, respectively in both the plots. These resonances arise from enhanced s-channel annihilation processes mediated by the SM particles, where the mediator mass is approximately twice the DM mass, leading to resonant enhancement and consequently reduced relic abundance.

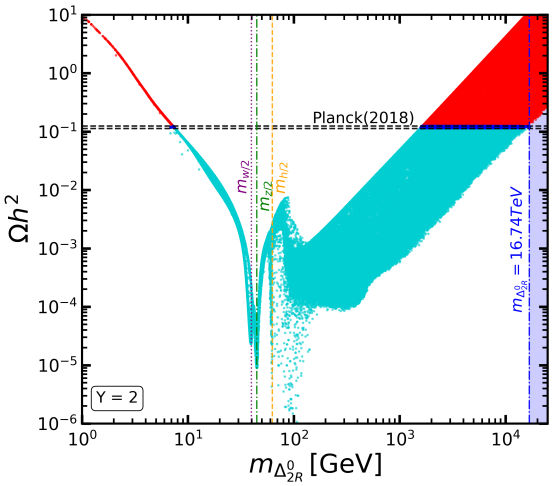

(a) Relic density of scalar DM as a function of its mass.

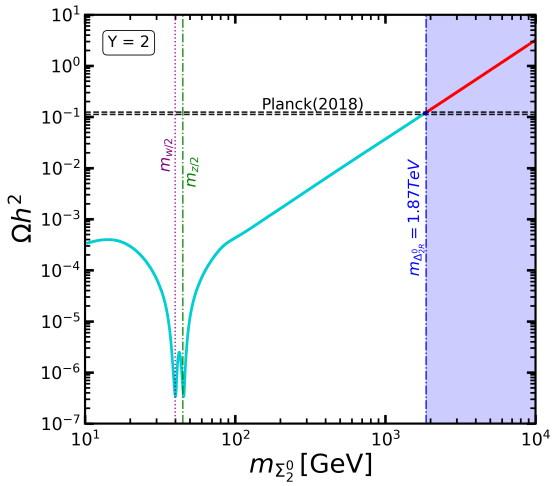

(b) Relic density of fermionic DM as a function of its mass.

FIG. 3: Comparison of relic density for scalar (left) and fermionic (right) DM candidates. The dark-turquoise and red points represent under- and over-abundant relic densities respectively. The black horizontal line shows the Planck 2018 limit on the DM relic density, and the blue points correspond to parameter values satisfying this constraint. The dips correspond to resonant annihilation near half the masses of the W, Z, and Higgs bosons.

The blue points satisfy the Planck limit with 3σ experimental range of DM. [1] $\Omega h^2 = 0.1126 - 0.1246$ (shown as the blue horizontal band with 3σ limit), demonstrating that the correct DM relic density can be achieved in specific mass ranges near these resonance regions. This behavior is characteristic of WIMP DM models, where the relic density is inversely proportional to the thermally averaged annihilation cross section $\langle\sigma v\rangle$. The mass range satisfying the Planck limit extends from **1.59 TeV to 16.74 TeV** for scalar and **1.81 TeV to 1.87 TeV** for fermion case. Comparing this with the Scotogenic case(doublet DM particle) fig. 2, we understand that the triplet has relatively less number of points satisfying relic abundance hence it is easier to probe the triplet case.

4.2. Direct Detection

Direct Detection (DD) experiments aim to observe the rare elastic scattering of galactic DM particles with nuclei in terrestrial detectors, measuring the small recoil energies (∼keV) deposited during these interactions. Fig. 4 displays the spin-independent WIMP-nucleon scattering cross-section $\sigma_{\rm SI}$ as a function of the triplet DM mass.

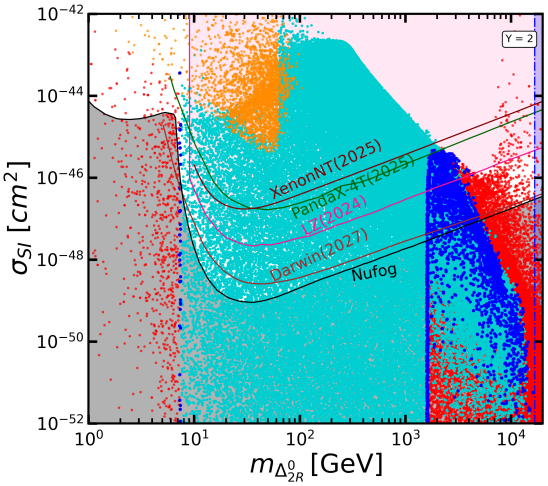

(a) Spin-independent WIMP–nucleon cross section for scalar triplet Δ^0 as a function of m_{Δ^0}.

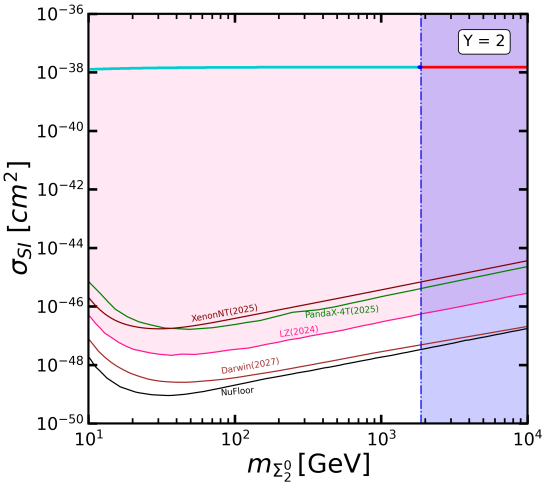

(b) Spin-independent WIMP–nucleon cross section for fermionic triplet Σ^0 as a function of m_{Σ^0}.

FIG. 4: Comparison of spin-independent WIMP–nucleon cross sections for scalar (left) and fermionic (right) triplet DM candidates. The color scheme is the same as in the previous figure, with darkorange points representing parameter regions that do not satisfy the Higgs invisible decay limit.

The darkturquoise(red) points represent parameter space with under(over) abundant relic density respectively, while blue points satisfy the Planck limit with 3σ experimental range of DM ($\Omega h^2 = 0.1126 - 0.1246$) [1]. The experimental exclusion bounds from current and

future direct detection experiments are shown: LZ 2024 [8] (pink), PandaX-4T [9] (green), and XenonNT 2025 [10] (maroon).

a. ***Scalar triplet*** Notably, the phenomenologically viable parameter space (blue points) lies well within the sensitivity reach of these experiments, Planck-compatible parameter space lie in range $m_{\Delta_2} \sim 1.59 - 5.70$ TeV, when becomes excluded by the LZ 2024 experiment.

The boundary of the scatter plot reflects the region where the cross–coupling parameters ($\lambda_{H\Delta}$ and $\lambda'_{H\Delta}$) reach their maximum allowed values. Along this boundary the cross section first increases with $m_{\Delta^0_{2R}}$ and then decreases. Towards the rightmost edge of the plot the number of blue points fulfilling the Planck relic density constraint diminishes rapidly. This behavior originates from the fact that at these high masses the cross–coupling constants approach their maximum values, which strongly modifies both the annihilation rate and the scattering amplitude. Consequently the allowed parameter space becomes increasingly narrow and the direct detection signal effectively vanishes at the far end of the scan. for the $Y = 2$ case, the scalar triplet is *complex*, allowing the presence of two independent Higgs–DM interaction terms. The finite contribution from the additional coupling parameter leads to spreading of viable relic density points in this scenario.

b. ***Fermion Triplet*** This value is several orders of magnitude above the current experimental upper bounds ($\sigma_{\rm SI} \lesssim 10^{-46}$ cm^2), implying that a Dirac fermion triplet with $Y = 2$ is excluded unless the Z-mediated interaction is suppressed, e.g. by splitting the neutral state into Majorana components or introducing inelastic scattering. Here, the neutral component couples to the Z boson, resulting in a very large SI cross-section, which is already excluded by current direct detection experiments.

5. FUTURE WORK

Furthermore, we plan to perform an ***indirect detection*** analysis for both models by plotting the annihilation cross section as a function of the DM candidate mass and comparing the results with current and future experimental limits. In addition, we aim to carry out a detailed ***collider phenomenology*** study, wherein we will analyze the relevant decay processes and compute the corresponding production cross sections for different parameter choices at various center-of-mass energies.

[1] Planck Collaboration, "Planck 2018 results. vi. cosmological parameters," *Astronomy Astrophysics* **641** (2020) A6, arXiv:1807.06209.

[2] P. Hut, "Limits on masses and number of neutral weakly interacting particles," *Physics Letters B* **69** no. 1, (1977) 85–88.

https://www.sciencedirect.com/science/article/pii/0370269377901393.

[3] B. W. Lee and S. Weinberg, "Cosmological lower bound on heavy-neutrino masses," *Phys. Rev. Lett.* **39** (Jul, 1977) 165–168. https://link.aps.org/doi/10.1103/PhysRevLett.39.165.

[4] E. W. Kolb and M. S. Turner, *The Early Universe*, vol. 69. Taylor and Francis, 5, 2019.

[5] G. Steigman, B. Dasgupta, and J. F. Beacom, "Precise relic wimp abundance and its impact on searches for dark matter annihilation," *Physical Review D* **86** no. 2, (July, 2012) . http://dx.doi.org/10.1103/PhysRevD.86.023506.

[6] P. Gondolo and G. Gelmini, "Cosmic abundances of stable particles: Improved analysis," *Nuclear Physics B* **360** no. 1, (1991) 145–179. https://www.sciencedirect.com/science/article/pii/0550321391904384.

[7] A. Arhrib, R. Benbrik, M. Chabab, G. Moultaka, M. C. Peyranere, L. Rahili, and J. Ramadan, "The Higgs Potential in the Type II Seesaw Model," *Phys. Rev. D* **84** (2011) 095005, arXiv:1105.1925 [hep-ph].

[8] **LZ** Collaboration, J. Aalbers *et al.*, "Dark Matter Search Results from 4.2 Tonne-Years of Exposure of the LUX-ZEPLIN (LZ) Experiment," *Phys. Rev. Lett.* **135** no. 1, (2025) 011802, arXiv:2410.17036 [hep-ex].

[9] **PandaX** Collaboration, Z. Bo *et al.*, "Dark Matter Search Results from 1.54 Tonne·Year Exposure of PandaX-4T," *Phys. Rev. Lett.* **134** no. 1, (2025) 011805, arXiv:2408.00664 [hep-ex].

[10] **XENON** Collaboration, E. Aprile *et al.*, "WIMP Dark Matter Search using a 3.1 tonne × year Exposure of the XENONnT Experiment," arXiv:2502.18005 [hep-ex].